

An Efficient Approach to Nowcasting the Time-varying Reproduction Number

 Bryan Sumalinab,^{a,b} Oswaldo Gressani,^a Niel Hens,^{a,c} and Christel Faes^a

Abstract: Estimating the instantaneous reproduction number (\mathcal{R}_t) in near real time is crucial for monitoring and responding to epidemic outbreaks on a daily basis. However, such estimates often suffer from bias due to reporting delays inherent in surveillance systems. We propose a fast and flexible Bayesian methodology to overcome this challenge by estimating \mathcal{R}_t while taking into account reporting delays. Furthermore, the method naturally takes into account the uncertainty associated with the nowcasting of cases to get a valid uncertainty estimation of the nowcasted reproduction number. We evaluate the proposed methodology through a simulation study and apply it to COVID-19 incidence data in Belgium.

Keywords: Epidemic; Nowcasting; Reporting delay; Reproduction number

(*Epidemiology* 2024;35: 512–516)

Submitted October 31, 2023; accepted March 26, 2024


From the ^aInteruniversity Institute for Biostatistics and Statistical Bioinformatics (I-BioStat), Data Science Institute (DSI), Hasselt University, Hasselt, Belgium; ^bDepartment of Mathematics and Statistics, College of Science and Mathematics, Mindanao State University - Iligan Institute of Technology, Iligan City, Philippines; and ^cCentre for Health Economics Research and Modelling Infectious Diseases (CHERMID), Vaccine & Infectious Disease Institute, Antwerp University, Antwerp, Belgium.

This work was supported by the ESCAPE project (101095619), co-funded by the European Union. Views and opinions expressed are however those of the author(s) only and do not necessarily reflect those of the European Union or European Health and Digital Executive Agency (HADEA). Neither the European Union nor the granting authority can be held responsible for them.

Disclosure: The authors report no conflicts of interest.

This manuscript was previously published in medRxiv: doi: <https://doi.org/10.1101/2023.10.30.23297251>.

R code for the simulation study can be found on GitHub at <https://github.com/bryansumalinab/Rnowcasting.git>, while the COVID-19 incidence data are available on the website of the Sciensano Research Institute (<https://epi-stat.sciensano.be/covid/>), accessed 11 April 2023).

 Supplemental digital content is available through direct URL citations in the HTML and PDF versions of this article (www.epidem.com).

Correspondence: Bryan Sumalinab, Interuniversity Institute for Biostatistics and Statistical Bioinformatics (I-BioStat), Data Science Institute (DSI), Hasselt University, Agoralaan Gebouw D, 3590 Diepenbeek, Belgium. E-mail: bryan.sumalinab@uhasselt.be.

Copyright © 2024 The Author(s). Published by Wolters Kluwer Health, Inc. This is an open-access article distributed under the terms of the Creative Commons Attribution-Non Commercial-No Derivatives License 4.0 (CCBY-NC-ND), where it is permissible to download and share the work provided it is properly cited. The work cannot be changed in any way or used commercially without permission from the journal.

ISSN: 1044-3983/24/354-512516

DOI: 10.1097/EDE.0000000000001744

The instantaneous reproduction number (\mathcal{R}_t) is one of the key infectious disease parameters that can be used to measure how likely a disease is to spread and to help direct effective management tactics during an epidemic. It is defined as the average number of infections caused by an infectious individual at a given time t . An \mathcal{R}_t value below 1 ($\mathcal{R}_t < 1$) indicates that the epidemic is waning, as each infected individual generates, on average, fewer than one new infection. Conversely, an \mathcal{R}_t value exceeding one ($\mathcal{R}_t > 1$) signifies a growing epidemic, with each case resulting in more than one additional infection. Therefore, the main goal is to implement interventions that would bring the \mathcal{R}_t value below 1 to control the spread of the epidemic. During the COVID-19 pandemic, the reproduction number has played a crucial role in informing policy decisions to mitigate the spread of the virus. Rapid transmission of the virus calls for timely updates that are essential to implement effective control measures. However, a problem arises as \mathcal{R}_t estimation methods typically rely on daily incidence counts that are frequently subject to reporting delays. Various factors contribute to these delays, such as testing backlogs, overwhelmed public health systems, communication and coordination challenges, and issues in data collection and reporting processes. Such delays have a direct impact on the reliability of \mathcal{R}_t estimates and hinder the timely assessment and response to the evolving epidemic situation.

Several methods have been developed to estimate \mathcal{R}_t from epidemiologic data. A recent paper by Gostic et al.¹ offers a comprehensive comparison of some established methodologies, discussing challenges and offering recommendations for accurate estimation of the reproduction number. An important issue mentioned by Gostic et al.¹ is the potential bias in estimating \mathcal{R}_t due to delays, for example, between confirmation and reporting of cases. A simple way to adjust for this is to sample from the delay distribution (assumed to be known) and subtract the sample from the observed data or by shifting estimates or observations backward by approximately the mean of the delay distribution. Gostic et al.¹ mentioned that these simple delay adjustments are less accurate in situations where delays are long and highly variable and when \mathcal{R}_t is rapidly changing. Moreover, these techniques do not adequately address the problem of right truncation, where recent cases are missing, that is, are not yet reported, rendering them unreliable for real-time \mathcal{R}_t estimation. For instance, subtracting a sample from the delay distribution may yield reliable \mathcal{R}_t

estimates for past time points but recent ones may be underestimated due to unreported cases.

One remedy to address the right truncation problem is by using nowcasting techniques.²⁻⁵ Their aim is to estimate the actual number of new cases by combining the (predicted) not-yet-reported cases and already-reported cases. Subsequently, the estimated or nowcasted cases can be used alongside established \mathcal{R}_t estimation methods to nowcast \mathcal{R}_t values. However, these procedures ignore the uncertainty in the nowcasted cases when estimating \mathcal{R}_t , yielding poor estimates of the credible interval (CI) for \mathcal{R}_t . Abbott et al.⁶ proposed a method that considers the appropriate uncertainty associated with reporting delays. However, the drawback of their approach is the added level of complexity in implementation and the extended computational time required. These can pose challenges for timely and daily updates on the epidemic situation. We propose to jointly estimate the time-varying lag in reporting and the time series of cases to directly derive the reproduction number (including uncertainty quantification) using a fast and flexible approach in a fully Bayesian framework. The proposed method directly models the delay feature in a data-driven way. In particular, we combine the Laplacian-P-splines method for nowcasting and estimation of \mathcal{R}_t proposed by Sumalinab et al.⁵ and Gressani et al.,⁷ respectively. R code used to implement the simulation study is available at <https://github.com/bryansumalinab/Rnowcasting.git>.

METHODS

Nowcasting

Let $y_{t,d}$ represent the incidence cases at time $t = 1, 2, \dots, T$ reported with a delay of $d = 0, 1, \dots, D$ days. Following van de Kassestele et al.,³ $y_{t,d}$ is assumed to follow a negative binomial distribution with mean $\mu_{t,d}$, overdispersion parameter ϕ , and variance $\mathbb{V}(y_{t,d}) = \mu_{t,d} + \mu_{t,d}^2/\phi$. The (log) mean number of cases is modeled using two-dimensional B-splines

$$\log(\mu_{t,d}) = \beta_0 + \sum_{j=1}^{K_T} \sum_{k=1}^{K_D} \theta_{j,k} b_j(t) b_k(d) + \sum_{l=1}^p \beta_l z_l(t, d),$$

where β_0 is the intercept, $b_j(\cdot)$ and $b_k(\cdot)$ are univariate (cubic) B-spline basis functions specified in the time and delay dimensions, respectively, and $z_l(t, d)$ represents day of the week effects with regression coefficients β_l .

To control the degree of roughness or smoothness of the fit, we adopt the penalized B-splines (P-splines) methodology proposed by Eilers and Marx.⁸ The idea is to specify a substantial number of B-spline basis functions and to counterbalance the implied flexibility by applying a roughness penalty on finite differences of adjacent B-spline coefficients. This penalty can then be translated into a Bayesian framework by specifying a (multivariate) Gaussian prior distribution for the B-spline coefficients.⁹ Moreover, Gamma

priors are assumed for the remaining model hyperparameters. Let $\xi = (\beta^T, \theta^T)^T$ denote the latent vector with regression coefficients $\beta = (\beta_0, \beta_1, \dots, \beta_p)^T$ and spline parameters $\theta = (\theta_{1,1}, \dots, \theta_{K_T,1}, \dots, \theta_{1,K_D}, \dots, \theta_{K_T,K_D})^T$. As shown in Sumalinab et al.,⁵ the Laplace approximation can be used to approximate the conditional posterior distribution of the latent vector ξ , yielding a Gaussian density with mean $\hat{\xi}$ and covariance matrix $\hat{\Sigma}$. From (1), the posterior mean of the nowcasted cases at time t can be derived as

$$\mathbb{E}(y_t) = \sum_{d=0}^D \mu_{t,d}.$$

We redirect the reader to the latter reference⁵ for full technical details regarding the sampling-free estimation scheme with Laplacian-P-splines.

Estimation of \mathcal{R}_t

For estimation of the time-varying reproduction number, we follow the work of Gressani et al.,⁷ where \mathcal{R}_t is expressed as the ratio of the mean incidence divided by the total infectiousness at time t ,¹⁰ given by

$$\mathcal{R}_t = \frac{\mathbb{E}(y_t)}{\sum_{s=1}^{t-1} \varphi_s y_{t-s}}$$

In the above equation, $\mathbb{E}(y_t)$ is the mean incidence at time t and $\varphi = (\varphi_1, \dots, \varphi_k)$ is the probability mass function of the serial interval distribution, where φ_s is defined as the probability that the serial interval, that is, the time elapsed between the onset of symptoms in an infector and the onset of symptoms in the secondary cases generated by that infector, is s days. Replacing $\mathbb{E}(y_t)$ and y_{t-s} with the mean nowcasted incidence at time t and $t - s$, respectively, the log of \mathcal{R}_t is modeled as

$$\log(\mathcal{R}_t) = \log \left(\sum_{d=0}^D \mu_{t,d} \right) + \log \left\{ \mathbb{I}(t = 1) + \left(\sum_{s=1}^{t-1} \varphi_s \left(\sum_{d=0}^D \mu_{t-s,d} \right) \right)^{-1} \mathbb{I}(2 \leq t \leq k) + \left(\sum_{s=1}^k \phi_s \left(\sum_{d=0}^D \mu_{t-s,d} \right) \right)^{-1} \mathbb{I}(k < t \leq T) \right\},$$

where $\mathbb{I}(\cdot)$ is an indicator function that $\mathbb{I}(A)$ equals 1 if A is true and 0 otherwise. The estimated time-varying reproduction number $\hat{\mathcal{R}}_t$ can be derived by replacing $\mu_{t,d}$ with the estimate $\hat{\mu}_{t,d}$ obtained from (1) and the variance of \mathcal{R}_t is approximated as

$$\mathbb{V}(\log(\mathcal{R}_t)) = \nabla_{\xi}^T \log(\mathcal{R}_t)|_{\xi=\hat{\xi}} \hat{\Sigma} \nabla_{\xi} \log(\mathcal{R}_t)|_{\xi=\hat{\xi}}.$$

Note that in the Laplacian-P-splines model, the posterior of $\log(\mathcal{R}_t)$ is approximated by a Gaussian distribution with mean $\log(\mathcal{R}_t)|_{\xi=\hat{\xi}}$ and variance $\mathbb{V}(\log(\mathcal{R}_t))$. Hence, quantile-based CIs for $\log(\mathcal{R}_t)$ can easily be obtained and subsequently, approximate CIs for \mathcal{R}_t by using the appropriate transformation. A detailed derivation of $\mathbb{V}(\log(\mathcal{R}_t))$ is given in the eAppendix; <http://links.lww.com/EDE/C132>.

RESULTS

Simulation Study

To assess the performance of our method, we conduct a simulation study and focus our evaluation on time T , that is, the nowcast date. We make certain assumptions on the serial interval distribution and the shape of the true time-varying reproduction number. The latter assumptions enable us to simulate daily case counts according to a negative binomial process. To incorporate reporting delays in the simulation, we assume fixed delay probabilities denoted by $p_0, p_1, p_2, \dots, p_D$. Subsequently, we generate samples from a multinomial distribution expressed as $(y_{t,0}, y_{t,1}, y_{t,2}, \dots, y_{t,D}) \sim \text{Multinomial}(y_t, p_0, p_1, p_2, \dots, p_D)$. This sample represents the reported number of cases for each (t, d) combination. Figure shows the target reproduction number to be estimated. We focus on several nowcast dates as represented by the dashed vertical lines in Figure with the following characteristics: (1) $T = 124$, start of the upward trend; (2) $T = 140$, increasing phase; (3) $T = 150$, local peak; (4) $T = 151$, start of the downward trend; (5) $T = 165$, decreasing phase; and (6) $T = 190$, stabilizing phase.

We consider several performance measures such as bias, absolute percentage error, CI coverage, CI width, and percentage of \mathcal{R}_t estimates falling below the target reproduction number ($\% \hat{\mathcal{R}}_t < \mathcal{R}_t$). We compute these metrics on the nowcast date, with the median bias, absolute percentage error, and CI width over 500 simulations. Besides assessing the performance of our approach, we also check the performance of the methodology proposed by Gressani et al.⁷ to estimate the instantaneous reproduction number assuming two different scenarios for the data stream input. A first scenario assumes that the data input solely relies on the reported incidence cases and ignores the nowcasted incidence. A second scenario uses the nowcasted incidence as data input. The former data stream ignores the reporting delays, while the latter takes these delays into account but ignores the uncertainty associated with the

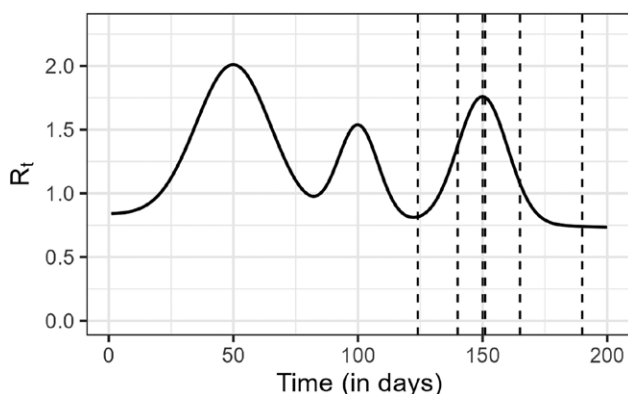


FIGURE. Target time-varying reproduction number with dashed vertical lines corresponding to different nowcast dates of interest.

delay dimension. In both scenarios, estimation of \mathcal{R}_t is carried out using the *estimR()* routine of the EpiLPS package.¹¹ To summarize, the simulation study allows to compare three models, namely \mathcal{M}_1 providing \mathcal{R}_t estimates using reported cases only, \mathcal{M}_2 providing \mathcal{R}_t estimates using nowcasted incidence data, and \mathcal{M}_3 , our new method that jointly models the delay and the time-varying reproduction number.

Simulation results are shown in Table 1 assuming no case is reported on the nowcast day. Results solely relying on the reported incidence (\mathcal{M}_1) show consistent negative bias and the largest percentage error across all scenarios. This indicates that the target \mathcal{R}_t is underestimated when using reported cases only, as expected. Furthermore, it exhibits the highest percentage error and the lowest coverage across all scenarios. On the other hand, when accounting for reporting delays, both \mathcal{M}_2 and \mathcal{M}_3 demonstrate similar performance in terms of bias and percentage error, suggesting that point estimates of \mathcal{R}_t are relatively close to each other. When \mathcal{R}_t is continuously increasing ($T = 140$) or decreasing ($T = 165$), the percentage error is slightly larger (around 14%–18% and 23%–29%, respectively) compared with other nowcast dates. Looking at the percentage of \mathcal{R}_t estimates falling below the target reproduction number ($\% \hat{\mathcal{R}}_t < \mathcal{R}_t$), point estimates are mostly below or above the target \mathcal{R}_t for increasing and decreasing trends, respectively. The width of the CI gets larger when the uncertainty linked to the delays is taken into consideration (\mathcal{M}_3), resulting in the highest level of coverage. However, neglecting this uncertainty (\mathcal{M}_2) yields a significant undercoverage, suggesting that the constructed CI often excludes the target reproduction number \mathcal{R}_t . Moreover, the CI is widest when \mathcal{R}_t is at the local peak ($T = 150$) or in its neighborhood ($T = 151$).

Additional simulation results are presented in the eAppendix; <http://links.lww.com/EDE/C132> assuming available data on the nowcast day. Specifically, we assume that 25% and 50% of the cases are reported on the nowcast day. The previously discussed findings in Table 1 remain consistent in the latter simulation scenarios. Furthermore, when examining the results in eTables 1 and 2; <http://links.lww.com/EDE/C132>, we observe that for \mathcal{M}_3 , the bias and percentage error are quite similar to those in Table 1 except when \mathcal{R}_t is decreasing ($T = 165$). There, we observe a decrease in bias and percentage error. This implies that our method performs well in terms of point estimation even when no data is available for the nowcast day. Moreover, the CI width is narrower and the coverage is closer to the nominal level. This is due to the fact that having more data on the nowcast day results in less uncertainty.

Real Data Application

We now apply our method to COVID-19 incidence data in Belgium for the year 2022. The raw data come from the website of the Sciensano Research Institute.¹² The data are truncated to a maximum delay of 5 days and we use the (discrete) serial interval distribution $\varphi = (0.344, 0.316, 0.168, 0.104, 0.068)$

TABLE 1. Performance Measures on the Nowcast Day With No Case Reported on the Nowcast Day and Delay Probabilities $(p_0, p_1, p_2, \dots, p_7) = (0.0, 0.30, 0.25, 0.15, 0.10, 0.10, 0.05, 0.05)$

	Bias	$\% \widehat{\mathcal{R}}_t < \mathcal{R}_t$	APE	95% CI Width	95% CI Coverage
<i>T</i> = 124					
\mathcal{M}_1	-0.580	99.600	71.190	0.194	9.600
\mathcal{M}_2	0.028	40.400	12.272	0.260	62.400
\mathcal{M}_3	-0.008	53.200	8.538	0.688	100.000
<i>T</i> = 140					
\mathcal{M}_1	-0.951	100.000	69.373	0.251	5.600
\mathcal{M}_2	-0.165	76.000	14.323	0.289	44.800
\mathcal{M}_3	-0.244	94.800	17.785	0.834	96.800
<i>T</i> = 150					
\mathcal{M}_1	-1.128	100.000	64.106	0.360	9.639
\mathcal{M}_2	0.013	48.193	9.640	0.237	40.562
\mathcal{M}_3	-0.102	70.400	8.618	1.092	99.600
<i>T</i> = 151					
\mathcal{M}_1	-1.113	100.000	63.449	0.339	5.622
\mathcal{M}_2	0.027	45.382	8.674	0.243	42.972
\mathcal{M}_3	-0.065	62.000	7.041	1.109	100.000
<i>T</i> = 165					
\mathcal{M}_1	-0.671	100.000	62.249	0.342	7.200
\mathcal{M}_2	0.255	3.600	23.670	0.135	18.800
\mathcal{M}_3	0.283	7.600	28.393	0.847	71.200
<i>T</i> = 190					
\mathcal{M}_1	-0.469	100.000	63.283	0.194	8.800
\mathcal{M}_2	0.025	40.800	7.748	0.154	66.000
\mathcal{M}_3	-0.011	58.800	6.967	0.453	100.000

APE indicates absolute percentage error.

from Gressani et al.⁷ Models are fitted with and without day of the week effects and different nowcast dates are compared. Results of these comparisons are available in eTable 3; <http://links.lww.com/EDE/C132> and results for the nowcast date of 31 July 2022 are presented in Table 2. The estimated \mathcal{R}_t curves for this nowcast date are presented in eFigures 1 and 2; <http://links.lww.com/EDE/C132>. We see in Table 2 that when accounting for reporting delays (\mathcal{M}_2 and \mathcal{M}_3), both with and without day of the week effects, the point estimates

are generally closer and higher compared with \mathcal{M}_1 . In addition, the \mathcal{M}_3 model has the widest CI. For the other nowcast dates (eTable 3; <http://links.lww.com/EDE/C132>), model \mathcal{M}_3 also has the widest CI. This translates into better interval coverage with values closer to the 95% nominal level. Moreover, incorporating day of the week effects for model \mathcal{M}_3 leads to a slightly narrower CI, which is also observed for the other nowcast dates presented in eTable 3; <http://links.lww.com/EDE/C132>.

TABLE 2. \mathcal{R}_t Estimates for the Nowcast Date on 31 July 2022 Using COVID-19 Data in Belgium and Assessment of Day of the Week Effects

	$\widehat{\mathcal{R}}_t$	95% CI Lower	95% CI Upper	CI Width
\mathcal{M}_1	0.780	0.634	0.960	0.326
\mathcal{M}_2 , week	0.899	0.747	1.081	0.335
\mathcal{M}_2 , no week	0.931	0.776	1.116	0.340
\mathcal{M}_3 , week	0.908	0.731	1.128	0.398
\mathcal{M}_3 , no week	0.912	0.720	1.155	0.435

Labels *week* and *no week* represent scenarios with and without day of the week effects, respectively.

Downloaded from <http://journals.lww.com/epidem> by BhDMf5ePHkav1ZEoun1tQIN4a+kLUEZqshH0d4XMI0hCwwCX1 AMN7YQp/1qH-D3D000Ry7T/SF14C3V/C4/OAV/pDDa8K2+Y+6H515KE= on 07/17/2024

CONCLUSION

This paper introduces a new method for nowcasting the instantaneous reproduction number taking into account reporting delays. The proposed model is fully Bayesian and uses Laplace approximations to posterior distributions as a surrogate to classic Markov chain Monte Carlo techniques to carry out inference. This yields efficient algorithms requiring low computational resources that are particularly well suited for near real-time monitoring of the time-varying reproduction number.

Simulation results show that relying solely on reported cases (\mathcal{M}_1) leads to a substantial underestimation of \mathcal{R}_t , as well as nonnegligible undercoverage. Using nowcasted incidence without accounting for the time lag uncertainty (\mathcal{M}_2) provides better point estimates of \mathcal{R}_t closer to the target value but still with moderate to strong undercoverage. However, directly nowcasting the reproduction number (\mathcal{M}_3) results in better uncertainty quantification as translated by an improved coverage. This can be attributed to wider CIs induced by the uncertainty in the reporting delay. Moreover, for the proposed \mathcal{M}_3 model, when data are available on the nowcast date, \mathcal{R}_t estimates become more accurate and CIs have close to nominal value coverage. Better CI coverage is desirable because it provides a more reliable estimate of the range in which the true value of the parameter (\mathcal{R}_t in our case) being estimated is expected to fall. Therefore, model \mathcal{M}_3 offers two primary advantages. First, it corrects for underestimation of \mathcal{R}_t . Second, it improves the CI coverage. The application to COVID-19 data shows that the new \mathcal{M}_3 model has the widest CIs as a result of accounting for the delay uncertainty. Although wider CIs may not always be desirable, simulation results indicate that this leads to improved coverage closer to the nominal level.

Through the use of Laplacian-P-splines, the methodology presented here shares the same skeleton as the EpiLPS

methodology⁷ and hence its integration in the latter ecosystem can be done without great difficulty. As such, we added nowcasting routines in the EpiLPS package to make them available in a user-friendly environment. It is also worth mentioning that using nowcasted case incidence data as an input to estimate \mathcal{R}_t (as in \mathcal{M}_2) transforms EpiLPS from a retrospective toolbox to a real-time toolbox, at least at the nowcasted time points.

REFERENCES

1. Gostic KM, McGough L, Baskerville EB, et al. Practical considerations for measuring the effective reproductive number, R_t . *PLoS Comput Biol*. 2020;16:e1008409.
2. Höhle M, an der Heiden M. Bayesian nowcasting during the STEC O104:H4 outbreak in Germany, 2011. *Biometrics*. 2014;70:993–1002.
3. van de Kasstele J, Eilers PHC, Wallinga J. Nowcasting the number of new symptomatic cases during infectious disease outbreaks using constrained P-spline smoothing. *Epidemiology*. 2019;30:737–745.
4. McGough SF, Johansson MA, Lipsitch M, Menzies NA. Nowcasting by Bayesian smoothing: a flexible, generalizable model for real-time epidemic tracking. *PLoS Comput Biol*. 2020;16:e1007735.
5. Sumalinab B, Gressani O, Hens N, Faes C. Bayesian nowcasting with Laplacian-P-splines. *MedRxiv*. 2023. doi:10.1101/2022.08.26.22279249.
6. Abbott S, Hellewell J, Thompson RN, et al; CMMID COVID modelling group. Estimating the time-varying reproduction number of SARS-CoV-2 using national and subnational case counts. *Wellcome Open Res*. 2020;5:112.
7. Gressani O, Wallinga J, Althaus CL, Hens N, Faes C. EpiLPS: a fast and flexible Bayesian tool for estimation of the time-varying reproduction number. *PLoS Comput Biol*. 2022;18:e1010618.
8. Eilers PHC, Marx BD. Flexible smoothing with B-splines and penalties. *Stat Sci*. 1996;11:89–121.
9. Lang S, Brezger A. Bayesian P-splines. *J Comput Graph Stat*. 2004;13:183–212.
10. Fraser C. Estimating individual and household reproduction numbers in an emerging epidemic. *PLoS One*. 2007;2:e758.
11. Gressani O. EpiLPS: A Fast and Flexible Bayesian Tool for Estimating Epidemiological Parameters. R package version 1.1.0. Available at: <https://cran.r-project.org/package=EpiLPS>. Accessed October 2023.
12. *Sciensano*. Available at: <https://epistat.sciensano.be/covid/>. Accessed 11 April 2023.